PHYSICAL REVIEW D **92,** 065014 (2015)

Thermodynamics of asymptotically safe theories

Dirk H. Rischke[1] and Francesco Sannino[2]

[1]*Institute for Theoretical Physics, Goethe University, Max-von-Laue-Strasse 1, D-60438 Frankfurt am Main, Germany*

[2]*CP[3]-Origins and the Danish Institute for Advanced Study, Danish IAS, University of Southern Denmark, Campusvej 55, DK-5230 Odense, Denmark*

(Received 6 June 2015; published 18 September 2015)

We investigate the thermodynamic properties of a novel class of gauge-Yukawa theories that have recently been shown to be completely asymptotically safe, because their short-distance behavior is determined by the presence of an interacting fixed point. Not only do all the coupling constants freeze at a constant and calculable value in the ultraviolet, their values can even be made arbitrarily small for an appropriate choice of the ratio N_c/N_f of fermion colors and flavors in the Veneziano limit. Thus, a perturbative treatment can be justified. We compute the pressure, entropy density, and thermal degrees of freedom of these theories to next-to-next-to-leading order in the coupling constants.

DOI: 10.1103/PhysRevD.92.065014 PACS numbers: 11.10.Wx

I. INTRODUCTION

Theories featuring gauge bosons, fermions, and scalars constitute the backbone of the Standard Model of particle interactions. This is to date one of the most successful models of nature. The recent discovery of asymptotically safe quantum field theories in four space-time dimensions [1], including their quantum-corrected potentials [2], widens the horizon of fundamental theories that can be used beyond the traditional asymptotically free paradigm [3,4]. The novelty resides in the occurrence of an exact interacting ultraviolet (UV) fixed point rather than a UV noninteracting fixed point, as it is the case for asymptotically free theories.

For the class of theories we will be investigating here a crucial property was unveiled in Ref. [1]: the Yukawa interactions, mediated by the scalars, compensate for the loss of asymptotic freedom due to the large number of gauged fermion flavors and therefore cure the subsequent growth of the gauge coupling. The further interplay of the gauge, Yukawa, and scalar interactions ensures that all couplings reach a stable interacting UV fixed point allowing for a *complete asymptotic safety* scenario in all couplings [1]. This is different from the *complete asymptotic freedom* scenario [5–7] where all couplings vanish in the UV; see Refs. [8,9] for recent studies.

The phase diagram including the scaling exponents of the theory was determined to the maximum known order in perturbation theory [1,2]. It was also shown in Ref. [2] that the scalar potential is stable at the classical and quantum level. Therefore these theories hold a special status: at arbitrarily short scales and without assuming additional symmetries they are fundamental according to Wilson's definition.

Having at our disposal new classes of fundamental theories one can use them to construct new dark-matter paradigms [10] or even support cosmic inflation [11]. It is therefore timely as well as theoretically and phenomenologically relevant to investigate, in a controllable manner, the thermodynamics of four-dimensional completely asymptotically safe theories.[1]

Because of the perturbative nature of the theory along the full energy range, our investigation of the thermal properties of asymptotically safe theories, besides being technically consistent, is also much better controlled than for QCD-like theories. This is so because at very low energies the theory is noninteracting and at very high energies the theory reaches an ultraviolet perturbative fixed point. Furthermore the value of the fixed point can be made arbitrarily small by changing the number of flavors and colors of the theory in the Veneziano-Witten limit. This allows us to consistently truncate the perturbative expansion by determining the range of convergence of the theory [1].

Going beyond the next-to-next-to-leading perturbative order investigated here is, however, challenging since perturbation theory must abide the Weyl consistency conditions [13,14]. These conditions relate couplings across different orders in perturbation theory for gauge-Yukawa theories featuring several couplings. For the Standard Model, the relevance of these conditions was proven in Ref. [15] and they have been further investigated in Ref. [13]. These conditions are nonconstraining for gauge theories with a single coupling such as QCD. A consistent mathematical counting scheme for gauge-Yukawa theories beyond the order investigated here has not yet been established. However, as explained above, by

[1]The thermodynamics of asymptotically free theories featuring perturbatively controllable and interacting IR fixed points has been investigated in Ref. [12] to the maximum known order in perturbation theory.

 © 2015 American Physical Society

changing the number of flavors and colors, and thereby the value of the ultraviolet fixed point, we have an extra handle, with respect to QCD, guaranteeing that the physical results are well within the range of convergence of the theory, at each given order, and therefore unaffected by higher-order corrections.

We organize this paper as follows. The theory and its salient zero-temperature properties are reviewed in Sec. II. This is followed by the determination of the asymptotically safe pressure to the leading order (LO), next-to-leading (NLO), and next-to-next-to-leading order (NNLO) in Sec. III. The entropy density of the system is determined and its properties are discussed in Sec. IV. The thermal degrees of freedom count for asymptotically safe theories is introduced and discussed in Sec. V. We offer our conclusions in Sec. VI where we also briefly discuss the impact of introducing a quark chemical potential. In the Appendixes we report the beta functions of the theory and further details of the computations of the pressure at the respective orders in perturbation theory.

II. ZERO-TEMPERATURE PHYSICS

Here we briefly review the salient aspects of the gauge-Yukawa system introduced in Ref. [1] such as the phase diagram of the theory and the expressions for the UV-safe trajectories away from the UV-stable fixed point. We will also provide the expressions for the running of the couplings along the globally defined UV-IR connecting line known as separatrix, or line of physics. Further quantities required for the subsequent thermodynamical analysis will also be reported.

The asymptotically safe theory suggested in Ref. [1] contains N_c^2-1 non-Abelian gauge fields A_μ^i, N_cN_f massless Dirac fermions ψ, and N_f^2 massless complex-valued scalars H. The theory has a local $SU(N_c)$ gauge symmetry and a global $U(N_f)_L \times U(N_f)_R$ chiral symmetry at the classical level. Because of the Adler-Bell-Jackiw axial anomaly the quantum global symmetry is $SU(N_f)_L \times SU(N_f)_R \times U(1)_V$. The left- and right-handed fermions live in the fundamental $(N_f,0)$ and $(0,N_f)$ representations of this symmetry group:

$$\psi_L \to \psi_L' = U_L\psi_L, \qquad \psi_R \to \psi_R' = U_R\psi_R, \tag{1}$$

while the scalars live in the adjoint (N_f,N_f^*) representation:

$$H \to H' = U_L H U_R^\dagger. \tag{2}$$

It is convenient to decompose the complex-valued $(N_f \times N_f)$ matrix H in terms of the generators T_a in the fundamental representation of $U(N_f)$, $a=0,\ldots,N_f^2-1$:

$$H = (S_a + iP_a)T_a, \tag{3}$$

where S_a are N_f^2 scalar and P_a are N_f^2 pseudoscalar fields. The Lagrangian reads

$$\begin{aligned}\mathcal{L} = &-\frac{1}{4}F^i_{\mu\nu}F_i^{\mu\nu} + \bar\psi i\not{D}\psi + \mathrm{Tr}(\partial_\mu H^\dagger \partial^\mu H)\\ &+ y(\bar\psi_L H\psi_R + \bar\psi_R H^\dagger \psi_L) - u\mathrm{Tr}(H^\dagger H)^2\\ &- v[\mathrm{Tr}(H^\dagger H)]^2,\end{aligned} \tag{4}$$

with the covariant derivative

$$D_\mu = \partial_\mu + igA_\mu^i t_i. \tag{5}$$

Here, g is the coupling constant of the non-Abelian gauge sector and $t_i, i=1,\ldots,N_c^2-1$, are the generators of $SU(N_c)$ in the fundamental representation.

At the classical level the theory counts four marginal couplings, the gauge coupling g, the Yukawa coupling y, the quartic scalar coupling u, and the double-trace scalar coupling v, which we write as

$$\begin{aligned}\alpha_g &= \frac{g^2N_c}{(4\pi)^2}, \qquad \alpha_y = \frac{y^2N_c}{(4\pi)^2},\\ \alpha_h &= \frac{uN_f}{(4\pi)^2}, \qquad \alpha_v = \frac{vN_f^2}{(4\pi)^2}.\end{aligned} \tag{6}$$

The appropriate powers of N_c and N_f in the normalization of the couplings allow us to take the Veneziano limit of the theory. Following Ref. [1] we will also use the shorthand notation $\beta_i \equiv \partial_t\alpha_i$, with $i=(g,y,h,v)$, for the beta functions of the respective couplings (6). It is convenient to introduce the continuous real parameter

$$\epsilon = \frac{N_f}{N_c} - \frac{11}{2} \tag{7}$$

in the Veneziano limit of large N_f and N_c, with the ratio N_f/N_c fixed. The relevant beta functions of the theory have been obtained in Ref. [14] in dimensional regularization, using the results of Refs. [16–18], and are summarized in Appendix A in the Veneziano limit.

For $\epsilon<0$ the theory is asymptotically free in the gauge sector while for $\epsilon>0$ it becomes a non-Abelian QED-like theory because asymptotic freedom is lost. It was shown in Ref. [1] that in this latter case the theory exhibits an interacting UV fixed point in all four couplings. This fixed point is controllable in perturbation theory, provided $0<\epsilon\ll 1$. The existence of such an interacting UV fixed point ensures that the theory is a fundamental one, i.e., it is valid at arbitrarily short and large distances. Furthermore, the scalar interactions are free from the triviality problem because of the presence of an interacting UV fixed point. Therefore, the elementary scalars are part of a Wilsonian fundamental theory.

After a lengthy study of the zeros of the theory [1], using the gauge-matter system (A1)–(A4), and including also the investigation of the stability of the associated classical and quantum scalar potential [2] one arrives at the only mathematically and physically acceptable fixed point accessible in perturbation theory:

$$\alpha_g^* = \frac{26}{57}\epsilon + \frac{23(75245 - 13068\sqrt{23})}{370386}\epsilon^2 + \mathcal{O}(\epsilon^3),$$
$$\alpha_y^* = \frac{4}{19}\epsilon + \left(\frac{43549}{20577} - \frac{2300\sqrt{23}}{6859}\right)\epsilon^2 + \mathcal{O}(\epsilon^3),$$
$$\alpha_h^* = \frac{\sqrt{23}-1}{19}\epsilon + \mathcal{O}(\epsilon^2),$$
$$\alpha_{v1}^* = -\frac{1}{19}(2\sqrt{23} - \sqrt{20+6\sqrt{23}})\epsilon + \mathcal{O}(\epsilon^2). \quad (8)$$

Here we give the analytic expression of the fixed point in an expansion in the small ϵ parameter.

The phase diagram of the theory was established in Ref. [1] at next-to-leading order accuracy and extended to the next-to-next-to-leading order in Ref. [2] where the effects from the running scalar couplings were considered. In order to keep the paper self-contained we summarize in Fig. 1 the phase diagram of the theory shown in Ref. [2]. In the left-hand panel we show the renormalization group (RG) trajectories for the (α_g, α_y) couplings, while in the right-hand panel the three-dimensional RG flow is illustrated, that includes also the coupling α_h. The two plots include the UV and IR fixed points. We have also indicated in the left panel the relevant and irrelevant directions dictated by the signs of the scaling exponents.

The IR fixed point is noninteracting and it is therefore located at the origin of coupling space. The thick red line connects the IR and UV fixed point and therefore is the UV-complete trajectory that we term the line of physics. The line of physics is also known as separatrix since it separates different regions of the theory in RG space. Along the line of physics the theory is noninteracting in the deep IR. The separatrix continues beyond the UV fixed point towards large couplings in the IR, leading to a strongly coupled theory presumably breaking conformality and chiral symmetry in the IR. The region of the RG phase diagram emanating from the UV-stable fixed point and leading to stable trajectories is known as the *UV critical surface*. Here this critical surface is one-dimensional [1] and it has a dynamical nature.

As mentioned above, the separatrix connects the UV fixed point with the Gaussian one and it agrees with the UV critical surface near the fixed point [1]. Although one can always determine numerically the globally defined separatrix, it is illuminating, in view of their use in the thermodynamical analysis, to consider an analytical approximation that is accurate in the limit of vanishing ϵ. This leads to the following relations among the couplings along the separatrix [2]:

$$\alpha_y = \frac{6}{13}\alpha_g,$$
$$\alpha_h = \frac{3}{26}(\sqrt{23}-1)\alpha_g,$$
$$\alpha_v = \frac{3}{26}\left(\sqrt{20+6\sqrt{23}} - 2\sqrt{23}\right)\alpha_g. \quad (9)$$

The one-dimensional nature of the line of physics is encoded in the fact that it is sufficient to know the running of the gauge coupling in order to determine the running of all the other couplings. The precise analytic running of the gauge coupling was determined in Ref. [2] and reads

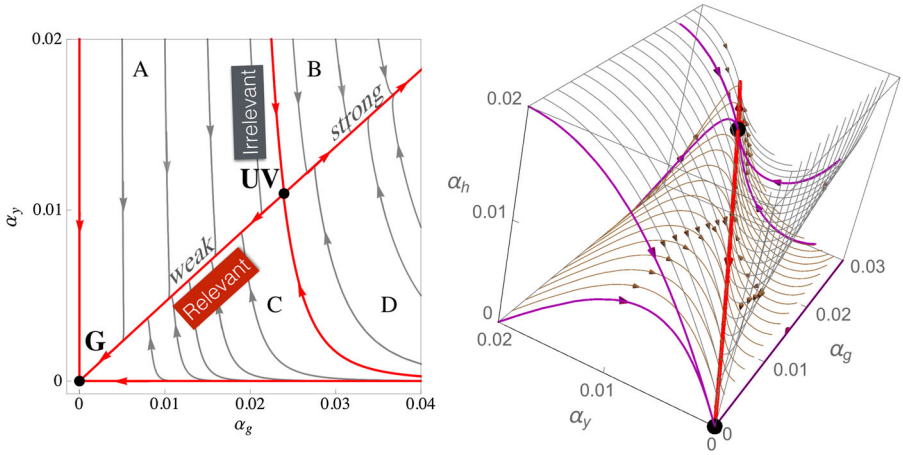

FIG. 1 (color online). Review of the phase diagram of Refs. [1,2]. The gauge-Yukawa subsector of couplings (α_g, α_y) is shown to leading order in the left-hand panel and the gauge-Yukawa-scalar subsector $(\alpha_g, \alpha_y, \alpha_h)$ at next-to-next-to-leading order accuracy in the right-hand panel for $\epsilon = 0.05$. Also shown are the UV and IR fixed points (dots) and the UV-safe trajectories (thick red line). A few trajectories are highlighted as thin magenta lines, and a few generic trajectories are shown as thin gray lines. Arrows point towards the IR. Further details can be found in Refs. [1,2].

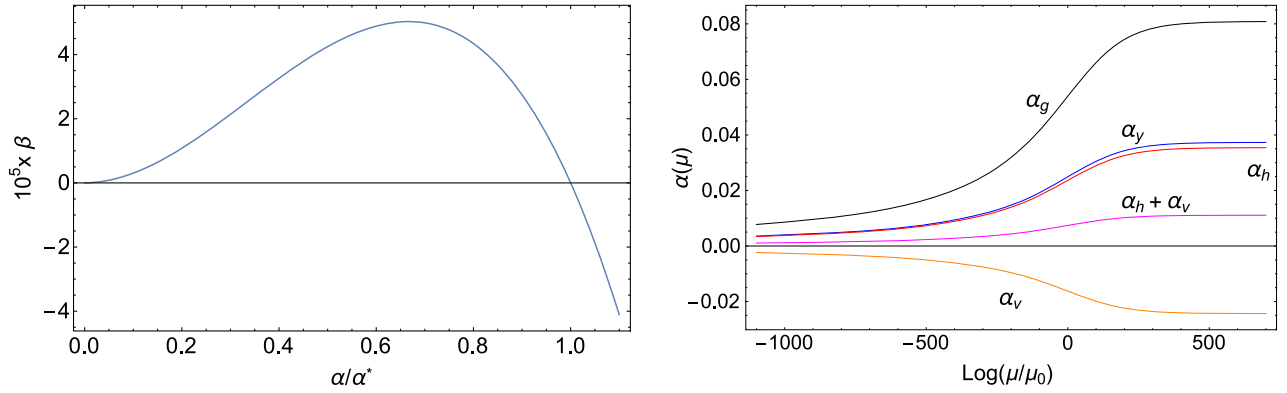

FIG. 2 (color online). Left panel: Gauge beta function along the line of physics displaying the characteristic asymptotically safe behavior. Right panel: From top to bottom the running of the gauge, Yukawa, single-trace, single-trace plus double-trace, and only single-trace coupling is shown along the line of physics. We have chosen $k = 1/2$ and $\epsilon = 0.1$.

$$\alpha_g(\mu) = \frac{\alpha_g^*}{1 + W(\mu)}, \tag{10}$$

where $W(\mu) \equiv W[z(\mu)]$ is the Lambert function satisfying the relation $z = W \exp W$ with

$$W = \frac{\alpha_g^*}{\alpha_g} - 1 \quad \text{and} \quad z = \left(\frac{\mu_0}{\mu}\right)^{\frac{4\epsilon}{3}\alpha_g^*} \left(\frac{\alpha_g^*}{\alpha_g^0} - 1\right) \exp\left(\frac{\alpha_g^*}{\alpha_g^0} - 1\right). \tag{11}$$

Here α_g^0 is the value of the gauge coupling at the scale μ_0, with μ/μ_0 ranging between 0 and ∞ and the gauge coupling ranging between $0 < \alpha_g^0 < \alpha_g^*$.

Inserting Eq. (10) into Eq. (9) yields an analytic description of the RG evolution of all couplings along the line of physics. This constitutes the zero-temperature information we need to establish the thermodynamical properties of the theory.

At asymptotically high energies $W(\mu)$ vanishes while it grows towards the infrared. It is convenient to fix α_g^0 via $\alpha_g^0 \equiv \alpha_g^*/(1 + k)$ with $k \in \mathbb{R}_+$, which in practice amounts to fixing the arbitrary renormalization reference scale μ_0 along the RG flow. As pointed out in Ref. [2] the value $k = 1/2$, i.e., $\alpha_g^0 = 2\alpha_g^*/3$, corresponds to an exact critical transition scale $\mu_0 = \Lambda_c$ above which the physics is dominated by the interacting UV fixed point and below which it is governed by the Gaussian IR fixed point. The interacting nature of the UV fixed point is expressed by the fact that it is approached as a power law in the renormalization scale

$$\alpha_g(\mu) \simeq \alpha_g^* + (\alpha_g^0 - \alpha_g^*)\left(\frac{\mu}{\bar{\mu}_0}\right)^{-\frac{104}{171}\epsilon^2}, \tag{12}$$

where $\bar{\mu}_0 = \mu_0(1 + \mathcal{O}(\epsilon))$. We have used Eq. (8) and that, in the deep-UV limit, the Lambert function approaches zero as

$$\lim_{\mu/\mu_0 \to \infty} W(\mu) \propto \left(\frac{\mu}{\mu_0}\right)^{-\frac{104}{171}\epsilon^2}. \tag{13}$$

There are several nice and distinctive features of the analytically controllable and completely asymptotically safe dynamics presented above. In particular, it constitutes an ideal laboratory to investigate thermodynamical properties of the theory that for certain aspects resembles $\mathcal{N} = 4$ theory. One of the similarities is the fact that along the line of physics all couplings are related. This is also a basic feature of $\mathcal{N} = 4$ theory due, however, to the high degree of space-time supersymmetry. In the nonsupersymmetric case the relations among the couplings are dynamical in nature being dictated by the dimension of the critical surface. In Fig. 2 we show in the left panel the beta function of the gauge coupling along the line of physics linking the Gaussian fixed point with the interacting UV fixed point. In the right panel the running of all couplings along the line of physics is shown using Eqs. (9) and (10). From the figure the completely asymptotically safe nature of the theory is evident. For the sake of completeness we mention that, at fixed N_c and large N_f, it has been argued [19] that an asymptotically safe theory can emerge without scalars and to leading order in $1/N_f$. Further physical properties of this intriguing possibility were investigated in Ref. [1].

III. ASYMPTOTICALLY SAFE THERMODYNAMICS

We will now study thermodynamical quantities of the theory to LO, NLO, and NNLO in the couplings. The details of the computation of the thermodynamic pressure for the gauge-Yukawa theory, that are valid for any number of colors and flavors and applicable as well to the entire phase diagram of the theory, are provided in Appendix B. We work here in the Veneziano limit and along the line of physics (9).

From Fig. 2 one can immediately see that there are three relevant energy regions with distinct dynamics: the one dominated by the Gaussian IR fixed point, i.e., $\mu \ll \Lambda_c$, the one dominated by the interacting UV fixed point $\mu \gg \Lambda_c$, and the crossover energy region for which $\mu \sim \Lambda_c$. By identifying, for example, the renormalization scale with the temperature, at zero chemical potential, we can test the thermodynamic properties of the asymptotically safe plasma along the entire line of physics.

A. Hot asymptotically safe pressure to leading order

Near the Gaussian IR fixed point the theory is noninteracting, and the ideal-gas limit applies. This constitutes the LO contribution along the entire line of physics. Specializing the results of Appendix B for the pressure to the Veneziano limit $(N_c, N_f \gg 1)$ at zero chemical potential, and normalizing it to the one of the gluons (in the same limit) we have

$$\frac{p_0}{p_{0,g}} = 1 + \frac{N_f^2}{N_c^2} + \frac{7}{4}\frac{N_f}{N_c}. \tag{14}$$

Here we notice that the ratio depends at most quadratically on N_f/N_c. We are, however, considering an expansion in $\epsilon = N_f/N_c - 11/2$ and therefore reexpress the result in terms of ϵ:

$$\frac{p_0}{p_{0,g}} = \frac{327}{8} + \frac{51}{4}\epsilon + \epsilon^2. \tag{15}$$

We note that already to this order the thermodynamical expression depends at most on ϵ^2 and that furthermore the ϵ expansion allows for a new handle on the thermodynamical expansion, which is absent for a generic gauge-Yukawa theory.

B. Hot asymptotically safe pressure to next-to-leading order

The previous LO expression for the pressure is exact at the IR fixed point because of its noninteracting nature. Since we choose to identify the renormalization scale with the temperature, this then occurs for very small temperatures, i.e., $\mu \equiv T \ll \Lambda_c$. However, when the temperature rises, the plasma starts feeling the various interactions. To NLO the pressure as a function of the temperature reads

$$\frac{p_{0+2}}{p_{0,g}} = \frac{327}{8} + \frac{51}{4}\epsilon + \epsilon^2 - 5\left[\alpha_g + (\alpha_v + 2\alpha_h)\left(\frac{11}{2} + \epsilon\right)^2\right] - \frac{25}{4}\left[\alpha_g\left(\frac{11}{2} + \epsilon\right) + \alpha_y\left(\frac{11}{2} + \epsilon\right)^2\right]. \tag{16}$$

Besides the trivial T^4 scaling which cancels between numerator and denominator, there is an additional temperature dependence due to the running of the couplings which are evaluated at the temperature T. In a conformal field theory, however, we can only consider ratios of scales or, equivalently, the couplings are measured in units of a reference value. Along the line of physics the natural choice for the reference scale is Λ_c, corresponding to a value of the gauge coupling, which is $2/3$ of its fixed-point value. This is the scale above which the physics is dominated by the UV fixed point, while below it is governed by the Gaussian IR one. This allows us to immediately determine the two limiting values of the pressure obtained for $T \ll \Lambda_c$ and for $T \gg \Lambda_c$.

For $T \ll \Lambda_c$ the physics is dominated, as already mentioned earlier, by the noninteracting fixed point and therefore the NLO pressure coincides with its ideal-gas expression:

$$\frac{p_{0+2}}{p_{0,g}} = \frac{327}{8} + \frac{51}{4}\epsilon + \epsilon^2 = 40.875 + 12.75\epsilon + \epsilon^2, \quad T \ll \Lambda_c. \tag{17}$$

However, for $T \gg \Lambda_c$, i.e., near or at the UV fixed point we can use the fixed-point values for the couplings (8), which yields

$$\frac{p_{0+2}}{p_{0,g}} = 40.875 - 84.6877\epsilon + \mathcal{O}(\epsilon^2), \quad T \gg \Lambda_c. \tag{18}$$

At zero temperature and chemical potential we have solved the theory to the maximum known order in perturbation theory that abides the Weyl consistency conditions. This implies that we know the gauge and Yukawa couplings to the second order in ϵ and the scalar couplings to the leading order in ϵ. This limits the expansion of the pressure in powers of ϵ to the next-to-leading order in ϵ. Interestingly, we observe a net drop of the pressure when normalized to the ideal-gas limit, valid in the deep IR, due to the interacting nature of the asymptotically safe plasma.

We can also determine the pressure along the entire line of physics by using Eqs. (9) and (10), where Eq. (16) reduces to

$$\frac{p_{0+2}}{p_{0,g}} = 40.875 + 12.75\epsilon + \epsilon^2 - (213.613 + 69.6094\epsilon + 5.75995\epsilon^2)\alpha_g(T), \quad \text{for any } T. \tag{19}$$

We use Eq. (10), replace the renormalization scale μ with T and the reference scale μ_0 with Λ_c, and write

$$\alpha_g(T) = \frac{\alpha_g^*}{1 + W(T)}. \tag{20}$$

From the knowledge of the functional dependence on T we deduce that the T^4 coefficient of the pressure decreases

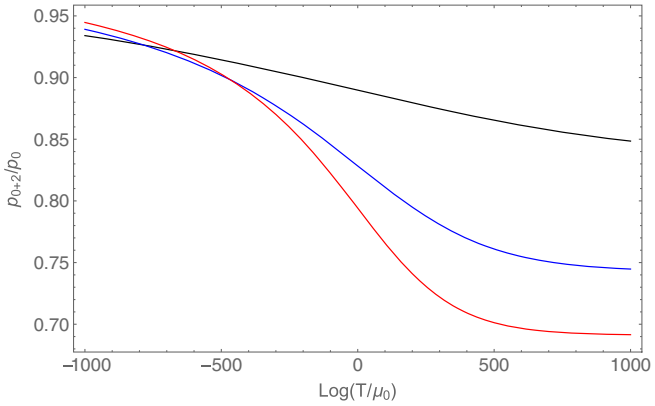

FIG. 3 (color online). Pressure normalized to the leading-order ideal-gas value, up to NLO corrections, as a function of the temperature. We have chosen $k = 1/2$, meaning that $\mu_0 = \Lambda_c$. From bottom to top ϵ assumes the values 0.08 (red line), 0.07 (blue line), and 0.05 (black line).

monotonically when the temperature increases. The theory assumes ideal-gas behavior only in the deep IR. This is different from the case of asymptotically free field theories where the ideal-gas limit is approached in the deep UV. From Fig. 3 we observe a decrease in the value of the pressure around Λ_c, now normalized to the ideal-gas limit, when increasing the temperature. By increasing ϵ the change in the pressure is more pronounced.

C. Hot asymptotically safe pressure to next-to-next-to-leading order

At this order we observe the emergence of nonanalytic contributions in the couplings. More specifically, the leading contributions will start at $\mathcal{O}(g^3)$ and $\mathcal{O}(u^{3/2}, v^{3/2})$. These come from the plasmon-ring diagrams [20] (cf. Fig. 7), and the detailed computation of their contribution to the pressure is given in Appendix C. The respective contribution to the pressure in the Veneziano limit reads

$$\frac{p_3}{p_{0,g}} = \frac{10}{\sqrt{3}}\alpha_g^{\frac{3}{2}}(15+2\epsilon)^{\frac{3}{2}} + \frac{5}{\sqrt{3}}(2\alpha_h+\alpha_v+\alpha_y)^{\frac{3}{2}}(11+2\epsilon)^2 = 150\sqrt{5}\alpha_g^{\frac{3}{2}} + \frac{605}{\sqrt{3}}(2\alpha_h+\alpha_v+\alpha_y)^{\frac{3}{2}} + \mathcal{O}(\epsilon^{\frac{5}{2}}). \quad (21)$$

Here we used the fact that all couplings are already of order ϵ; see Eq. (8). Along the line of physics (9) this reduces to

$$\frac{p_3}{p_{0,g}} = 704.061\alpha_g(T)^{\frac{3}{2}} + \mathcal{O}(\epsilon^{\frac{5}{2}}). \quad (22)$$

Besides the fact that the contribution is nonanalytic in ϵ we learn that it starts at $\mathcal{O}(\epsilon^{3/2})$ and that it is positive, differently from the NLO contribution which is negative and starts at $O(\epsilon)$. Near the UV fixed point, i.e., at temperatures $T \gg \Lambda_c$, it assumes the value

$$\frac{p_3}{p_{0,g}} = 216.899\epsilon^{\frac{3}{2}} + \mathcal{O}(\epsilon^{\frac{5}{2}}), \quad T \gg \Lambda_c. \quad (23)$$

The full pressure to $\mathcal{O}(\epsilon^{3/2})$ at nonzero temperature, zero chemical potential, in the Veneziano limit, and along the line of physics reads

$$\frac{p_{0+2+3}}{p_{0,g}} = 40.875 + 12.75\epsilon - 213.613\alpha_g(T) + 704.061\alpha_g(T)^{\frac{3}{2}} + \mathcal{O}(\epsilon^2), \quad \text{for any } T. \quad (24)$$

The pressure normalized to the noninteracting limit is shown in the two panels of Fig. 4 for different values of ϵ. For the plot on the left the values for ϵ are, from bottom to top, 0.05 (black line), 0.03 (blue line), and 0.01 (red line), while the values for the solid curves on the right are 0.08 (red line),

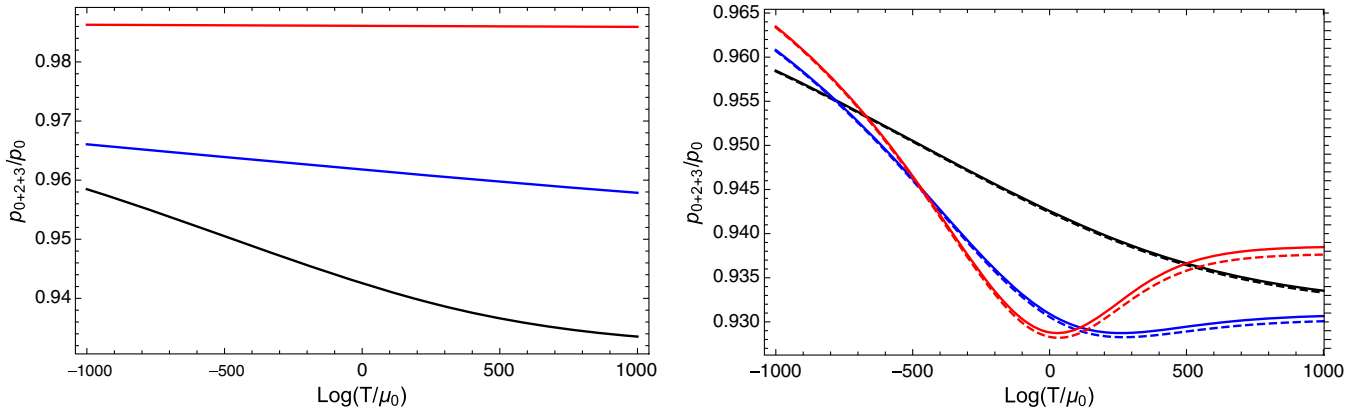

FIG. 4 (color online). Pressure up to NNLO, normalized to its LO value, as a function of the temperature. We have chosen $k = 1/2$ meaning that $\mu_0 = \Lambda_c$. Left panel: The values for ϵ are, from bottom to top, 0.05 (black line), 0.03 (blue line), and 0.01 (red line). Right panel: The ϵ values for the solid curves are 0.08 (red line), 0.07 (blue line), and 0.05 (black line). We kept some of the higher-order corrections in ϵ for the respective dashed curves.

0.07 (blue line), and again, for reference, 0.05 (black line). For the dashed curves we retain some of the higher-order corrections in ϵ in order to gain an estimate on their order of magnitude. These come by retaining all the powers in ϵ from Eqs. (19) and (21). Overall the analysis shows that we have good control of the perturbative expansion up to NNLO terms. Because the NNLO corrections to the pressure are positive, the total value of the pressure increases with respect to its NLO value, but not with respect to its LO value, when approaching the UV fixed point. Furthermore, the normalized pressure starts developing a minimum near Λ_c when ϵ increases above the value 0.05.

The decrease of the pressure normalized to the one of the ideal gas is not guaranteed to be monotonic because of the effects of the NNLO corrections. However, within the realm of perturbation theory this quantity globally decreases, i.e.,

$$\Delta p_{\rm norm} \equiv \frac{p_{0+2+3}(T \ll \Lambda_c)}{p_0} - \frac{p_{0+2+3}(T \gg \Lambda_c)}{p_0} = 2.384\epsilon - 5.306\epsilon^{\frac{3}{2}} \geq 0, \tag{25}$$

provided that $\epsilon < 0.202$. This is guaranteed by the fact that the radius of convergence of the expansion is, at zero temperature, $\epsilon < 0.11$ [1], and it is even smaller at nonzero temperature.

IV. ASYMPTOTICALLY SAFE ENTROPY

Another important quantity to determine is the entropy density of the system, which is related to the pressure via

$$s = \frac{dp}{dT}. \tag{26}$$

Given that in the present system, and along the line of physics, the pressure can be written as a function of only one coupling we have

$$p = f(\alpha_g(T))\frac{\pi^2}{90}T^4. \tag{27}$$

In the noninteracting gas $f(\alpha_g(T))$ is the number of boson degrees of freedom plus $7/4$ times the number of Weyl fermions. The entropy density normalized to the one of an ideal gas of gluons reads

$$\frac{s}{s_{0,g}} = \frac{1}{2(N_c^2-1)}\left[f + \frac{\beta(\alpha_g)}{4}\frac{df}{d\alpha_g}\right] = \frac{p}{p_{0,g}} + \frac{\beta(\alpha_g)}{4}\frac{d(p/p_{0,g})}{d\alpha_g} = \frac{p}{p_{0,g}} + \frac{1}{4}\frac{d(p/p_{0,g})}{d\ln T}, \tag{28}$$

with $\beta(\alpha_g) = d\alpha_g/d\ln\mu$, where $\mu = T$, is the gauge beta function along the line of physics. We have used the fact that $f = 2(N_c^2-1)p/p_{0,g}$. Because the beta functions vanish at a fixed point we have that at the IR and UV fixed points the normalized entropy density agrees with the normalized fixed-point pressure and therefore

$$\frac{s_{\rm IR}}{s_{0,g}} = \lim_{T/\Lambda_c\to 0}\frac{p}{p_{0,g}} = \frac{f_{\rm IR}}{2N_c^2} = 1 + \frac{N_f^2}{N_c^2} + \frac{7}{4}\frac{N_f}{N_c} = 40.875 + 12.75\epsilon + \epsilon^2, \tag{29}$$

$$\frac{s_{\rm UV}}{s_{0,g}} = \lim_{T/\Lambda_c\to\infty}\frac{p}{p_{0,g}} = \frac{f_{\rm UV}}{2N_c^2} = \frac{f(\alpha_g^*)}{2N_c^2} = 40.875 - 84.6877\epsilon + 216.899\epsilon^{3/2} + \mathcal{O}(\epsilon^2). \tag{30}$$

Away from the fixed points the normalized entropy density and pressure differ by the quantity

$$\frac{s}{s_{0,g}} - \frac{p}{p_{0,g}} = \frac{\beta(\alpha_g)}{4}\frac{d(p/p_{0,g})}{d\alpha_g}, \tag{31}$$

which is directly proportional to the beta function of the theory. This behavior is different, for example, from the case of $\mathcal{N} = 4$ theory where the beta function vanishes identically.

Using the NNLO expression for the pressure from Eq. (24) we deduce

$$\frac{s_{0+2+3}}{s_{0,g}} - \frac{p_{0+2+3}}{p_{0,g}} = -53.4033\frac{d\alpha_g(T)}{d\ln T}[1 - 4.94395\alpha_g(T)^{\frac{1}{2}}]. \tag{32}$$

This contribution being directly proportional to the gauge beta function along the line of physics from Fig. 2 it is clear

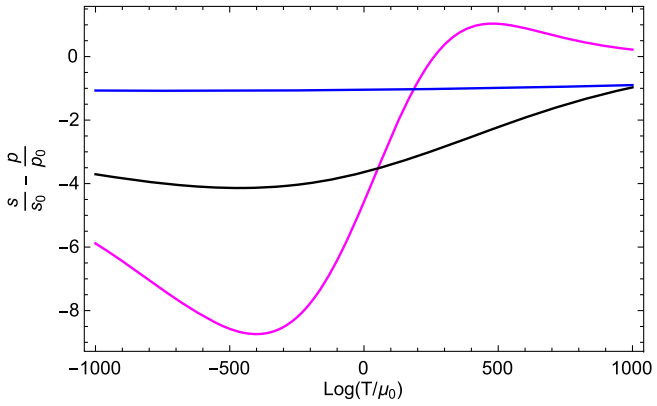

FIG. 5 (color online). We show the difference between the entropy density normalized to its leading-order ideal-gas value minus the similarly normalized pressure, in units of 10^{-6}, up to NNLO corrections as a function of the temperature. We have chosen $k = 1/2$ meaning that $\mu_0 = \Lambda_c$ and from bottom to top ϵ assumes the values 0.07 (magenta line), 0.05 (black line), and 0.03 (blue line).

that it is suppressed compared to the term directly proportional to the normalized pressure and therefore decreases from the IR to the UV. In Fig. 5 we show the difference in entropy density and pressure both normalized with respect to the ideal-gas limit, rather than the ideal gas of gluons. The difference is simply an overall numerical factor.

We learn that the entropy density normalized to the ideal-gas limit decreases overall from the IR to the UV with the dominant piece, in perturbation theory, given by the normalized pressure. However it does not decrease monotonically.

V. ASYMPTOTICALLY SAFE THERMAL DEGREES OF FREEDOM

The free energy density $\mathcal{F}(T) = -p(T)$ can be used to count the physical degrees of freedom of the theory at different energy scales. The temperature probes the relevant degrees of freedom by exciting them. Therefore the function

$$f(T) = -\frac{\mathcal{F}(T)}{T^4}\frac{90}{\pi^2} = \frac{p(T)}{T^4}\frac{90}{\pi^2} \tag{33}$$

is a possible candidate to count these degrees of freedom. Alternatively one can use the T^3 coefficient of the opportunely normalized entropy density, i.e., $f + df/4d\ln T$. The two definitions coincide at fixed points. We can now count, for the first time, the thermal degrees of freedom along the entire line of physics of a completely asymptotically safe field theory. Up to an overall normalization the result is the one presented in Fig. 4. It shows that the thermal degrees of freedom decrease from the infrared to the ultraviolet, albeit not monotonically. In the deep infrared, i.e., for the cold field theory, we have of course the ideal-gas result

$$f_{\rm IR} = \lim_{T\to 0} f(T) = 2(N_c^2 - 1) + 2N_f^2 + \frac{7}{2}N_f N_c, \tag{34}$$

that in the Veneziano limit reads

$$\frac{f_{\rm IR}}{2N_c^2} = 1 + \frac{N_f^2}{N_c^2} + \frac{7}{4}\frac{N_f}{N_c}. \tag{35}$$

By construction this function coincides with Eq. (14) and provides the overall normalization.

Interestingly we discover

$$f_{\rm IR} \geq f_{\rm UV}, \tag{36}$$

for the classes of asymptotically safe theories investigated here with

$$f_{\rm UV} = \lim_{T\to\infty} f(T). \tag{37}$$

This demonstrates that the inequality $f_{\rm IR} \leq f_{\rm UV}$ that has been conjectured to be valid for asymptotically free field theories [21] does not apply to asymptotically safe field theories.[2] The fact that this function decreases in the present case is due to the fact that the theory becomes interacting in the UV while it is free from interactions in the deep infrared. On the other hand the a-theorem is satisfied as shown in Ref. [14].

VI. CONCLUSIONS

We have computed relevant thermodynamic properties of nonsupersymmetric four-dimensional completely asymptotically safe field theories [1] up to NNLO. Because of the completely asymptotically safe nature of the theories that have been investigated here the coupling constants freeze at a constant and calculable value in the UV. Furthermore, their value can be made arbitrarily small in the Veneziano limit because of the existence of a continuous control parameter. This has justified a perturbative determination of the vacuum and in-medium properties of the theories investigated here. In this work we have determined the pressure and entropy density of these theories to next-to-next-to-leading order. We find that because of the nature of the interactions, both the pressure and the entropy density normalized to their respective noninteracting ideal-gas values decrease when going from the infrared to the ultraviolet.

After this initial investigation several novel avenues can be explored such as the response of completely asymptotically safe theories to the introduction of different kinds of chemical potentials. Here, we would just like to remark on one interesting physical phenomenon. For the sake of simplicity, we assume that there is a single chemical potential μ_q associated to fermion number conservation. Similarly to QCD, at nonzero μ_q and sufficiently low temperature, the theory features a color-superconducting phase, because of attractive one-gauge field exchange interactions near the Fermi surface [25]. Because of the Pauli principle, fermion Cooper pairs must form in channels which are totally antisymmetric in color-flavor-spin space. To be definite, let us focus on Cooper pairs in the antisymmetric spin-zero channel. Such pairs must then be either completely antisymmetric or completely symmetric in both color and flavor. In QCD, the one-gluon exchange interaction is attractive in the antisymmetric color-antitriplet channel, which requires also an antisymmetric

[2]The inequality has not been proven even for asymptotically free theories, but it was shown to be consistent with known results and then used to derive constraints for several strongly coupled, vectorlike gauge theories. The correct counting of the infrared degrees of freedom, with respect to the inequality, for the important case of an $SU(2) = Sp(2)$ gauge theory with fermions in the fundamental representation was first performed correctly in Ref. [22]. The conjecture has been used also for chiral gauge theories [23,24].

wave function in flavor space. In principle, this is different in the gauge-Yukawa theories studied here: the scalar fields can mediate attractive interactions also for symmetric representations in color space, which in turn demands a symmetric flavor wave function. However, whether this actually happens requires a more quantitative study, since a repulsive interaction in the symmetric color channel may destroy the pairing. Nevertheless, the phenomenon of color superconductivity (in an antisymmetric color channel) in these theories is robust: *any* attractive interaction, no matter how small, will destabilize the Fermi surface and lead to the formation of Cooper pairs. Therefore, Cooper pairs will form except right at the Gaussian IR fixed point, i.e., at $T=\mu=0$. In the perturbative regime, i.e., for $\epsilon \ll 1$, the system is a BCS superconductor, with a gap which is exponentially small in the coupling. For $\epsilon \ll 1$, i.e., $N_c \sim 2N_f/11$, a chiral-density wave phase is not expected to occur; this would require $N_c \gtrsim 1000 N_f$ [26].

ACKNOWLEDGMENTS

D. H. R. acknowledges the hospitality of the heavy-ion theory group at the University of Jyväskylä, the Helsinki Institute of Physics, and the University of Southern Denmark, where part of this work was done. The work of F. S. is partially supported by the Danish National Research Foundation under Grant No. DNRF:90.

APPENDIX A: BETA FUNCTIONS

In the large-N limit, the perturbative renormalization group equations for the couplings (6) have been obtained in Ref. [14] in dimensional regularization, also using the results of Refs. [16–18]. In terms of Eq. (7) they are given by

$$\begin{aligned}\beta_g = {}& \frac{4}{3}\epsilon\alpha_g^2 + \left[\left(25+\frac{26}{3}\epsilon\right)\alpha_g - \frac{1}{2}(11+2\epsilon)^2\alpha_y\right]\alpha_g^2 \\ & + \left[\left(\frac{701}{6}+\frac{53}{3}\epsilon-\frac{112}{27}\epsilon^2\right)\alpha_g^2 - \frac{27}{8}(11+2\epsilon)^2\alpha_g\alpha_y \right. \\ & \left. + \frac{1}{4}(11+2\epsilon)^2(20+3\epsilon)\alpha_y^2\right]\alpha_g^2, \end{aligned} \tag{A1}$$

$$\begin{aligned}\beta_y = {}& \alpha_y[(13+2\epsilon)\alpha_y - 6\alpha_g] \\ & + \alpha_y\left[\frac{20\epsilon-93}{6}\alpha_g^2 + (49+8\epsilon)\alpha_g\alpha_y \right. \\ & \left. - \left(\frac{385}{8}+\frac{23}{2}\epsilon+\frac{\epsilon^2}{2}\right)\alpha_y^2 - 4(11+2\epsilon)\alpha_y\alpha_h + 4\alpha_h^2\right], \end{aligned} \tag{A2}$$

$$\beta_h = -(11+2\epsilon)\alpha_y^2 + 4\alpha_h(\alpha_y+2\alpha_h), \tag{A3}$$

$$\beta_v = 12\alpha_h^2 + 4\alpha_v(\alpha_v+4\alpha_h+\alpha_y), \tag{A4}$$

for $\beta_g, \beta_y, \beta_h$, and β_v up to (3,2,1,1)-loop order, respectively. In the terminology of Ref. [1] we refer to this as the NNLO approximation. The NLO approximation corresponds to the approximation in which the (2,1,0,0)-loop terms for $\beta_g, \beta_y, \beta_h$, and β_v are retained. As discussed in Ref. [1], this ordering of perturbation theory is also favored by the Weyl consistency conditions [13,14,27].

APPENDIX B: EXPLICIT COMPUTATION OF THE THERMODYNAMICAL PROPERTIES

In this Appendix we determine the thermodynamical quantities of the theory to LO and NLO in the couplings. For a perturbative calculation of the pressure we need to identify the interaction vertices in Eq. (4). The gauge sector will be analogous to QCD, so we shall simply use the results from Ref. [20]. For the Yukawa interaction and the self-interaction of the scalar, however, we will be more explicit. We therefore decompose the Yukawa interaction term $\sim y$ in Eq. (4) with the help of Eq. (3) and the definition of the projectors onto right- and left-handed chirality, $P_{R,L} \equiv (1 \pm \gamma_5)/2$,

$$\bar\psi_L H \psi_R + \bar\psi_R H^\dagger \psi_L = \bar\psi T_a \psi S_a + i\bar\psi T_a \gamma_5 \psi P_a. \tag{B1}$$

In order to compute the self-interaction terms $\sim u, v$ of the scalar field H, we utilize the decomposition (3), the orthogonality relation

$$\mathrm{Tr}(T_a T_b) = \frac{1}{2}\delta_{ab}, \tag{B2}$$

and the (anti)commutation relations for the generators of $U(N_f)$,

$$\begin{aligned}\{T_a, T_b\} &= d_{abc}T_c, \\ [T_a, T_b] &= i f_{abc} T_c, \end{aligned} \tag{B3}$$

where d_{abc} (f_{abc}) are the totally (anti)symmetric structure constants of $U(N)$. We obtain

$$\mathrm{Tr}(H^\dagger H) = \frac{1}{2}(S_a^2 + P_a^2), \tag{B4}$$

$$\begin{aligned}\mathrm{Tr}(H^\dagger H)^2 = {}& \frac{1}{24}(d_{abn}d_{cdn} + d_{acn}d_{bdn} + d_{adn}d_{bcn}) \\ & \times (S_a S_b S_c S_d + P_a P_b P_c P_d) \\ & + \frac{1}{4}(d_{abn}d_{cdn} + f_{acn}f_{bdn} + f_{adn}f_{bcn}) \\ & \times S_a S_b P_c P_d. \end{aligned} \tag{B5}$$

1. Pressure to LO

To LO, the pressure of the theory (4) is that of an ultrarelativistic ideal gas of $N_c^2 - 1$ gauge fields, $N_c N_f$

Dirac fermions, and $2N_f^2$ scalars. At temperature T, and if we assume a common chemical potential μ_q for all fermions (associated to net-fermion number conservation), we have

$$p_0(T,\mu_q) = p_{0,g}(T) + p_{0,f}(T,\mu_q) + p_{0,H}(T), \tag{B6}$$

where [20]

$$\begin{aligned} p_{0,g}(T) &= 2(N_c^2-1)\frac{\pi^2}{90}T^4, \\ p_{0,f}(T,\mu_q) &= 2N_cN_f\left(\frac{7}{4}\frac{\pi^2}{90}T^4 + \frac{\mu_q^2T^2}{12} + \frac{\mu_q^4}{24\pi^2}\right), \\ p_{0,H}(T) &= 2N_f^2\frac{\pi^2}{90}T^4. \end{aligned} \tag{B7}$$

2. Pressure to NLO

The NLO contribution to the pressure,

$$\begin{aligned} p_2(T,\mu_q) = p_{2,g}(T) + p_{2,gf}(T,\mu_q) + p_{2,Hf}(T,\mu_q) \\ + p_{2,H}(T), \end{aligned} \tag{B8}$$

has a diagrammatic representation in terms of the two-loop diagrams shown in Fig. 6. The first term in Eq. (B8) is the contribution from the self-interaction of the gauge fields and gauge fields with ghosts; cf. Figs. 6(a)–6(c). It reads [20]

$$p_{2,g}(T) = -g^2N_c(N_c^2-1)\frac{T^4}{144}. \tag{B9}$$

The second term in Eq. (B8) is the contribution from the fermion loop [Fig. 6(d)], where the fermion interacts with a gauge field. This reads [20]

$$p_{2,gf}(T,\mu_q) = -g^2(N_c^2-1)N_f\left(\frac{5T^4}{576} + \frac{\mu_q^2T^2}{32\pi^2} + \frac{\mu_q^4}{64\pi^4}\right). \tag{B10}$$

The third term in Eq. (B8) is the contribution from the fermion loop [Figs. 6(e) and 6(f)], where the fermion interacts either with a scalar or a pseudoscalar field. It turns out that both contributions are identical. The calculation proceeds analogous to the one for Fig. 6(d). The result is, up to a prefactor, identical to Eq. (B10):

$$p_{2,Hf}(T,\mu_q) = -y^2N_f^2N_c\left(\frac{5T^4}{576} + \frac{\mu_q^2T^2}{32\pi^2} + \frac{\mu_q^4}{64\pi^4}\right). \tag{B11}$$

The last term in Eq. (B8) receives contributions from the vertices $\sim u$ and $\sim v$ in Eq. (4):

$$p_{2,H}(T) = p_{2,u}(T) + p_{2,v}(T). \tag{B12}$$

We first compute the latter. With the help of Eq. (B4) we write

$$\begin{aligned} &-v[\mathrm{Tr}(H^\dagger H)]^2 \\ &\quad = -\frac{v}{4}(S_aS_aS_bS_b + 2S_aS_aP_bP_b + P_aP_aP_bP_b). \end{aligned} \tag{B13}$$

In order to produce a double-bubble diagram of the type shown in Fig. 6(g), either (i) we can tie a leg $\sim S_a$ together with the other leg $\sim S_a$ (then we must tie S_b together with

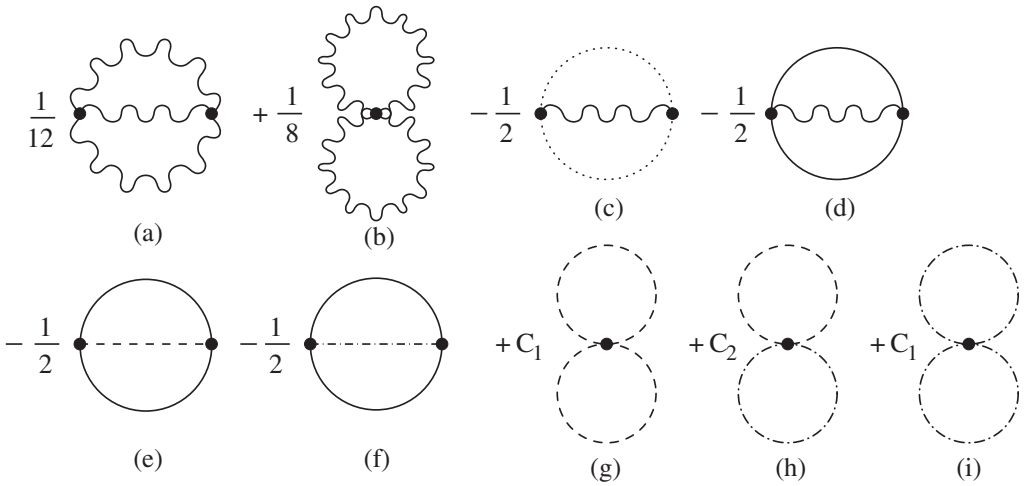

FIG. 6. Two-loop contributions to the pressure. Diagrams (a)–(d) are the same as in QCD; gauge fields are represented by wavy lines, ghosts by dotted lines, and fermions by solid lines. Diagrams (e) and (f) are the two-loop contributions in a Yukawa theory where fermions interact with scalar (dashed line) and pseudoscalar fields (dash-dotted line). Diagrams (g)–(i) are the two-loop contributions arising from the self-interaction of the scalar field H, decomposed in terms of scalars and pseudoscalars. The combinatorial factors C_1 and C_2 are implicitly computed in the text but will not be needed explicitly.

S_b), or (ii) we can tie a leg $\sim S_a$ together with one of the two legs $\sim S_b$ (then the other leg $\sim S_a$ must be tied together with the other leg $\sim S_b$). Case (i) corresponds to a Hartree-type routing of internal indices and produces an overall factor of N_f^4, because there are N_f^2 scalar fields running in each of the two loops. Case (ii) corresponds to a Fock-type routing of internal indices and produces an overall factor of N_f^2, because all indices are tied together in a way that there is effectively only one loop in the index a. Overall, we obtain a factor of $N_f^2(N_f^2+2)$. The same can be repeated for the pseudoscalar contribution [Fig. 6(i)] with the same result, as nothing distinguishes the two types of fields in the absence of chiral symmetry breaking. The remaining diagram is the one with one scalar and one pseudoscalar loop; cf. Fig. 6(h). Here, the factor is [with the factor 2 from Eq. (B13)] simply $2N_f^4$. Each double-bubble diagram is proportional to the square of a tadpole which, for massless particles, has the value $T^2/12$ [20]. Altogether we obtain

$$p_{2,v}(T) = -vN_f^2(N_f^2+1)\frac{T^4}{144}. \tag{B14}$$

We now compute $p_{2,u}(T)$. We first consider the contribution to the diagrams in Figs. 6(g) and 6(i), corresponding to the first two lines in Eq. (B5). The three different ways to tie legs together to form a double-bubble diagram can be written in terms of a combination of Kronecker deltas, so that the prefactor becomes

$$\begin{aligned}&\frac{1}{24}(d_{abn}d_{cdn}+d_{acn}d_{bdn}+d_{adn}d_{bcn})\\&\quad\times(\delta_{ab}\delta_{cd}+\delta_{ac}\delta_{bd}+\delta_{ad}\delta_{bc})\\&=\frac{1}{8}(d_{aan}d_{bbn}+2d_{abn}d_{abn})\\&=\frac{1}{4}N_f(2N_f^2+1),\end{aligned} \tag{B15}$$

where we have used $d_{aan}=\sqrt{2}N_f^{3/2}\delta_{n0}$ (a sum over a is implied) and $d_{abn}d_{abn}=N_f(N_f^2+1)$. [This can be proven using the relationship $d_{ijk}d_{ijk}=(N_f^2-1)(N_f^2-4)/N_f$, $i,j,k=1,\ldots,N_f^2-1$, for the symmetric structure constants of $SU(N_f)$.] Now we consider the contribution to the diagram in Fig. 6(h), arising from the last two lines in Eq. (B5). Here, there is only one way to tie the legs together:

$$\begin{aligned}&\frac{1}{4}(d_{abn}d_{cdn}+f_{acn}f_{bdn}+f_{adn}f_{bcn})\delta_{ab}\delta_{cd}\\&\quad=\frac{1}{4}(d_{aan}d_{ccn}+2f_{acn}f_{acn})=\frac{1}{2}N_f(2N_f^2-1),\end{aligned} \tag{B16}$$

where we have used the relationship $f_{abn}f_{abn}\equiv f_{ijk}f_{ijk}=N_f(N_f^2-1)$. Putting all this together [remembering that Eq. (B15) is multiplied by a factor of 2, for scalar and pseudoscalar contributions], we obtain

$$\begin{aligned}p_{2,u}(T)&=-\frac{u}{2}N_f(2N_f^2+1+2N_f^2-1)\frac{T^4}{144}\\&=-2uN_f^3\frac{T^4}{144}.\end{aligned} \tag{B17}$$

Adding the contributions (B9)–(B12) [which is a sum of Eqs. (B14) and (B17)], the complete NLO contribution to the pressure is

$$\begin{aligned}&p_2(T,\mu_q)\\&=-[g^2(N_c^2-1)N_c+vN_f^2(N_f^2+1)+2uN_f^3]\frac{T^4}{144}\\&\quad-[g^2(N_c^2-1)N_f+y^2N_f^2N_c]\left(\frac{5T^4}{576}+\frac{\mu_q^2T^2}{32\pi^2}+\frac{\mu_q^4}{64\pi^4}\right)\end{aligned} \tag{B18}$$

Using the properly normalized large N_c and N_f couplings and taking the Veneziano limit we arrive at

$$\begin{aligned}\frac{p_2(T,\mu_q)}{p_{0,g}(T)}&=-5\left[\alpha_g+(\alpha_v+2\alpha_h)\frac{N_f^2}{N_c^2}\right]\\&\quad-5\left(\alpha_g\frac{N_f}{N_c}+\alpha_y\frac{N_f^2}{N_c^2}\right)\left(\frac{5}{4}+\frac{9}{2\pi^2}\frac{\mu_q^2}{T^2}+\frac{9}{4\pi^4}\frac{\mu_q^4}{T^4}\right).\end{aligned} \tag{B19}$$

Trading N_f/N_c for ϵ we have

$$\begin{aligned}&\frac{p_2(T,\mu_q)}{p_{0,g}(T)}\\&=-5\left[\alpha_g+(\alpha_v+2\alpha_h)\left(\frac{11}{2}+\epsilon\right)^2\right]-5\left[\alpha_g\left(\frac{11}{2}+\epsilon\right)\right.\\&\quad\left.+\alpha_y\left(\frac{11}{2}+\epsilon\right)^2\right]\left(\frac{5}{4}+\frac{9}{2\pi^2}\frac{\mu_q^2}{T^2}+\frac{9}{4\pi^4}\frac{\mu_q^4}{T^4}\right).\end{aligned} \tag{B20}$$

We observe the explicit dependence on the couplings of the theory.

APPENDIX C: PRESSURE TO NNLO

To NNLO, the pressure at nonzero temperature and chemical potential receives contributions from the so-called plasmon-ring diagrams [20]; cf. Fig. 7. The leading contributions of these plasmon-ring diagrams are $\sim O(g^3)$ and $\sim O(u^{3/2},v^{3/2})$. These are calculated in the following. There is a plasmon ring for the gauge field A_μ^i and one for the scalar field H:

$$p_3(T,\mu_q)=p_{3,g}(T,\mu_q)+p_{3,H}(T,\mu_q). \tag{C1}$$

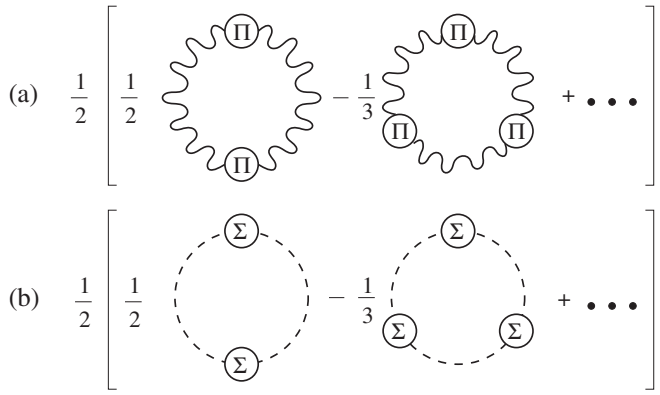

FIG. 7. Plasmon-ring contributions to the pressure. The diagrams (a) are the same as in QCD, while the diagrams (b) are the plasmon-ring contribution from the scalar field H (shown only for a scalar S_a; the one for a pseudoscalar P_a has the same value).

The contribution from the gauge field [Fig. 7(a)] is the same as in QCD [20]; thus

$$p_{3,g}(T,\mu_q) = (N_c^2-1)\frac{Tm_g^3(T,\mu_q)}{12\pi}, \tag{C2}$$

with the electric screening mass of the gauge field [20]

$$m_g^2(T,\mu_q) = g^2\left[N_c\frac{T^2}{3} + N_f\left(\frac{T^2}{6}+\frac{\mu_q^2}{2\pi^2}\right)\right]. \tag{C3}$$

In analogy to Eq. (C2), the plasmon-ring contribution from the scalar field H reads

$$p_{3,H}(T,\mu_q) = 2N_f^2\frac{Tm_H^3(T,\mu_q)}{12\pi}, \tag{C4}$$

where

$$m_H^2(T,\mu_q) \equiv \Sigma(0,0) \tag{C5}$$

is the screening mass of the scalar field; $\Sigma(0,0)$ is the zero-Matsubara frequency, zero-momentum limit of the corresponding one-loop self-energy. The prefactor $2N_f^2$ takes into account that we have $2N_f^2$ (pseudo)scalar degrees of freedom. Thus, we only need to compute $\Sigma(0,0)$ for one of these fields, say the scalar field S_0. In general, the one-loop self-energy of the scalar field can be computed by functional differentiation of the two-loop contribution to the pressure with respect to the scalar propagator $\mathcal{S}$ [20]:

$$\Sigma \sim -2\frac{\delta p_2}{\delta \mathcal{S}}. \tag{C6}$$

This corresponds to amputating a scalar propagator in the diagrams shown in Fig. 6. Obviously, only the diagrams (e), (g), and (h) can contribute to Σ. The contribution from the fermion loop in Fig. 6(e) is

$$\begin{aligned}\Sigma_f(Q) &= y^2T\sum_n\int\frac{\mathrm{d}^3\vec{k}}{(2\pi)^3}\mathrm{Tr}[\mathcal{G}(K)T_0\mathcal{G}(K-Q)T_0]\\ &= \frac{y^2N_c}{2}\int\frac{\mathrm{d}^3\vec{k}}{(2\pi)^3}\left\{(1-\hat{k}\cdot\hat{p})\left[\frac{n_F(k-\mu_q)-n_F(p-\mu_q)}{q_0+k-p}-\frac{n_F(k+\mu_q)-n_F(p+\mu_q)}{q_0-k+p}\right]\right.\\ &\left.-(1+\hat{k}\cdot\hat{p})\left[\frac{1-n_F(k-\mu_q)-n_F(p+\mu_q)}{q_0+k+p}-\frac{1-n_F(k+\mu_q)-n_F(p-\mu_q)}{q_0-k-p}\right]\right\}.\end{aligned} \tag{C7}$$

Here, $\vec{p}\equiv\vec{k}-\vec{q}$, $\hat{k}=\vec{k}/k$, and $n_F(k\mp\mu_q)=[e^{(k\mp\mu_q)/T}+1]^{-1}$ is the Fermi-Dirac distribution for (anti)particles. After renormalization of the vacuum contribution and taking the limit $q_0=0,\vec{q}\to 0$, we obtain

$$\Sigma_f(0,0) = \frac{y^2N_c}{4}\left(\frac{T^2}{3}+\frac{\mu_q^2}{\pi^2}\right). \tag{C8}$$

The contributions from the double-bubble diagrams [Figs. 6(g) and 6(h)] can be decomposed into two parts, one proportional to the vertex v and one to the vertex u. For the first one, we have from the Hartree-type routing of internal indices in Fig. 6(g) a factor $2\times N_f^2$ (a factor 2 because one can open either one of the two tadpoles) and from the Fock-type routing a factor $2\times 2=4$ (one factor of 2 because the Fock-type diagram appears twice relative to the Hartree-type one and one factor of 2 because one can open either one of the two tadpoles). Finally, we have a factor $2\times 1=2$ from the diagram in Fig. 6(h) (one factor of 2 because this type of diagram appears twice relative to Hartree-type one and a factor of 1 because functional differentiation only opens the scalar tadpole). The remaining tadpole is the same, since there is nothing that distinguishes scalar from pseudoscalar fields. After renormalization of the tadpole (which then is equal to $T^2/12$) we obtain

$$\Sigma_v = -2\left(-\frac{v}{4}\right)(2N_f^2+4+2)\frac{T^2}{12} = v(N_f^2+3)\frac{T^2}{12}. \tag{C9}$$

Finally, we compute the contribution from the diagrams in Figs. 6(g) and 6(h) proportional to the vertex u. Here we go back to the left-hand side of Eq. (B15). Amputating a scalar propagator (corresponding to the zeroth scalar field S_0) means that any two of the indices a, b, c, d may take the value 0. For symmetry reasons we may restrict ourselves to the first factor $\delta_{ab}\delta_{cd}$ in the second set of parentheses and multiply the result by a factor of 3. Now we have either $a = b = 0$ or $c = d = 0$. This gives

$$\begin{aligned}&\frac{1}{8}(d_{abn}d_{cdn} + d_{acn}d_{bdn} + d_{adn}d_{bcn})(\delta_{a0}\delta_{b0}\delta_{cd} + \delta_{c0}\delta_{d0}\delta_{ab})\\&= \frac{1}{4}(d_{aan}d_{00n} + 2d_{a0n}d_{a0n}) = \frac{1}{2}\left(N_f + \frac{2}{N_f}N_f^2\right)\\&= \frac{3}{2}N_f. \end{aligned} \tag{C10}$$

We also need to consider Eq. (B16). Here, only the indices a, b can take the value 0, and thus we have

$$\begin{aligned}&\frac{1}{4}(d_{abn}d_{cdn} + f_{acn}f_{bdn} + f_{adn}f_{bcn})\delta_{a0}\delta_{b0}\delta_{cd}\\&= \frac{1}{4}d_{00n}d_{ccn} = \frac{1}{2}N_f. \end{aligned} \tag{C11}$$

Putting everything together, we have

$$\Sigma_u = 2uN_f\frac{T^2}{12}. \tag{C12}$$

Adding Eqs. (C8), (C9), and (C12), we finally get

$$m_H^2(T, \mu_q) \equiv [v(N_f^2 + 3) + 2uN_f]\frac{T^2}{12} + \frac{y^2N_c}{4}\left(\frac{T^2}{3} + \frac{\mu_q^2}{\pi^2}\right). \tag{C13}$$

[1] D. F. Litim and F. Sannino, J. High Energy Phys. 12 (2014) 178.
[2] D. F. Litim, M. Mojaza, and F. Sannino, arXiv:1501.03061.
[3] D. J. Gross and F. Wilczek, Phys. Rev. Lett. **30**, 1343 (1973).
[4] H. D. Politzer, Phys. Rev. Lett. **30**, 1346 (1973).
[5] D. J. Gross and F. Wilczek, Phys. Rev. D **8**, 3633 (1973).
[6] T. P. Cheng, E. Eichten, and L. F. Li, Phys. Rev. D **9**, 2259 (1974).
[7] D. J. E. Callaway, Phys. Rep. **167**, 241 (1988).
[8] B. Holdom, J. Ren, and C. Zhang, J. High Energy Phys. 03 (2015) 028.
[9] G. F. Giudice, G. Isidori, A. Salvio, and A. Strumia, J. High Energy Phys. 02 (2015) 137.
[10] F. Sannino and I. M. Shoemaker, Phys. Rev. D **92**, 043518 (2015).
[11] N. G. Nielsen, F. Sannino, and O. Svendsen, Phys. Rev. D **91**, 103521 (2015).
[12] M. Mojaza, C. Pica, and F. Sannino, Phys. Rev. D **82**, 116009 (2010).
[13] I. Jack and C. Poole, J. High Energy Phys. 01 (2015) 138.
[14] O. Antipin, M. Gillioz, E. Mølgaard, and F. Sannino, Phys. Rev. D **87**, 125017 (2013).
[15] O. Antipin, M. Gillioz, J. Krog, E. Mølgaard, and F. Sannino, J. High Energy Phys. 08 (2013) 034.
[16] M. E. Machacek and M. T. Vaughn, Nucl. Phys. **B222**, 83 (1983).
[17] M. E. Machacek and M. T. Vaughn, Nucl. Phys. **B236**, 221 (1984).
[18] M. E. Machacek and M. T. Vaughn, Nucl. Phys. **B249**, 70 (1985).
[19] C. Pica and F. Sannino, Phys. Rev. D **83**, 035013 (2011).
[20] J. I. Kapusta and C. Gale, *Finite-Temperature Field Theory: Principles and Applications* (Cambridge University Press, Cambridge, England, 2006).
[21] T. Appelquist, A. G. Cohen, and M. Schmaltz, Phys. Rev. D **60**, 045003 (1999).
[22] F. Sannino, Phys. Rev. D **79**, 096007 (2009).
[23] T. Appelquist, A. G. Cohen, M. Schmaltz, and R. Shrock, Phys. Lett. B **459**, 235 (1999).
[24] T. Appelquist, Z. y. Duan, and F. Sannino, Phys. Rev. D **61**, 125009 (2000).
[25] M. G. Alford, A. Schmitt, K. Rajagopal, and T. Schfer, Rev. Mod. Phys. **80**, 1455 (2008).
[26] E. Shuster and D. T. Son, Nucl. Phys. **B573**, 434 (2000).
[27] I. Jack and H. Osborn, Nucl. Phys. **B343**, 647 (1990).